Molecular Biotechnology (2023) 65:1764–1776
https://doi.org/10.1007/s12033-023-00678-2

ORIGINAL PAPER

Anticancer and Biological Effects of Some Natural Compounds and Theoretical Investigation of them Against RdRP of SARS-COV-2: In Silico and In Vitro Studies

Jing Zhang[1,2] · Jingyu Feng[1] · Yang Li[1] · Jiguo Wang[1] · Panyan Mo[1] · Changguo Luo[1]

Received: 16 October 2022 / Accepted: 18 January 2023 / Published online: 13 February 2023

Abstract

In this study, Skullcapflavone I and Skullcapflavone II molecules showed good inhibitory activities against α-glucosidase and sorbitol dehydrogenase enzymes with IC50 values of 102.66 ± 8.43 and 95.04 ± 11.52 nM for α-glucosidase and 38.42 ± 3.82 and 28.81 ± 3.26 µM for sorbitol dehydrogenase. The chemical activities of Skullcapflavone I and Skullcapflavone II against α-glucosidase and sorbitol dehydrogenase were assessed by conducting the molecular docking study. The anticancer activities of the compounds were examined against SW-626, SK-OV-3, OVCAR3, and Caov-3 cell lines. The chemical activities of Skullcapflavone I and Skullcapflavone II against some of the expressed surface receptor proteins (estrogen receptor, EGFR, androgen receptor, and GnRH receptor) in the mentioned cell lines were investigated using in silico calculations. Moreover, the activity of the compounds against RNA polymerase of SARS-COVE-2 was also assessed using the molecular modeling study. These compounds created strong contacts with the enzymes and receptors. The considerable binding affinity of the compounds to the enzymes and proteins showed their ability as inhibitors. Furthermore, even at modest dosages, these substances markedly reduced the viability of ovarian cancer cells. Additionally, the viability of ovarian cancer cells was significantly decreased by a 300 µM dosage of all compounds. Antiovarian cancer results of Skullcapflavone I on SK-OV-3, SW-626, OVCAR3, and Caov-3 were 63.14, 1.55, 19.42, and 52.04 µM, respectively. Also, cytotoxicity results of Skullcapflavone II on SK-OV-3, SW-626, OVCAR3, and Caov-3 were 5.18, 21.44, 33.87, and 72.66 µM, respectively.

Keywords Natural compounds · α-glucosidase · Sorbitol dehydrogenase · In silico study · Cytotoxicity

Introduction

Flavone compounds are natural molecules of the benzopyran group, constituting a significant class of oxygen heterocycles that are extensively distributed in the plant kingdom as secondary metabolites. These natural compounds protect plant cells from UV radiation and attract insects to participate and pollinate in interactions with soil microbes. Due to their widespread presence in vegetables and fruits, they are also precious as antioxidant compounds in human cells [1, 2].

The α-glucosidases play a significant role in the lysis of α-glucopyranoside bonds in disaccharide molecules and oligosaccharide molecules to release monosaccharide compounds that get absorbed in the body [3]. A homotetrameric Zn-enzyme called sorbitol dehydrogenase (SDH) functions in the polyol metabolic pathway. Aldose reductase and SDH are the two enzymes that make up the polyol pathway. Using NAD^+ and NADPH as co-factors, this process changes the sugar alcohol intermediate sorbitol from the glucose molecule to the fructose molecule [4].

The fifth-leading cause of cancer-related death is ovarian cancer (OC), which is the deadliest malignancy in women. It is among the 10 most common types of cancer in women in Turkey. Often known as the silent killer, OC often goes undiagnosed until it is in an advanced stage because of its vague symptoms, making it difficult to treat. Treatment of patients with advanced OC usually includes cyto-reducing surgery and combination chemotherapy [5]. Chloride ions separate from the positively charged platinum ion when

✉ Changguo Luo
zhangjingtongxun@163.com

[1] Department of Oncology, Shenzhen Bao'an Traditional Chinese Medicine Hospital, Shenzhen 518000, China

[2] Department of Oncology, The First Clinical Medical College of Guangzhou University of Traditional Chinese Medicine, Guangzhou, China

the medication cisplatin is carried into cells. The charged platinum ion then binds to cellular DNA, RNA, and proteins and prevents transcription, translation, replication, and DNA repair. In the latest data of the American National Cancer Institute (NIH), it is stated that 10–20% of all cancer patients use cisplatin at some time during their treatment. However, drug resistance that occurs reduces the effectiveness of cisplatin. The development of new strategies to overcome intrinsic and acquired resistance to chemotherapy is critical in the effective treatment of OC and other types of cancer [6].

The role of the majority of the proteins or enzymes in the body is finalized by their relevant substrate or biomolecules to complete their functionality [7]. Comprehending the way substrate and related proteins interact can give necessary details for biologists. Molecular docking analysis is an adaptable approach that can provide such details and be conducted for choosing enzymatic substrates. By performing the molecular modeling method, the experimental results could be additionally assessed [8]. By using this strategy, the potential interactions between the ligands and enzymes or proteins could be examined at an atomic level [9]. The computational approaches can easily reduce the time-consuming for pharma products [10] and the price that has to be paid for that [11]. The molecular docking method has gained substantial consideration as a drug design tool. Additionally, the drug product procedure could be simplified by comprehending the docking process and forecasting drug goals.

Materials and Methods

Molecular Docking Study and Binding Free Energy Calculation

In this study were used alpha glucosidase (PDB ID: 5KZW) and human sorbitol dehydrogenase (PDB ID: 1PL7). As the chemical and naturally derived compounds have approved anticancer activities [12, 13], the anticancer activity of Skullcapflavone I and Skullcapflavone II were assessed against SW-626, SK-OV-3, OVCAR3, and Caov-3 cell lines. The surface receptors that are over expressed in the studied cell lines were investigated by applying molecular modeling. Estrogen receptor (PDB ID: 3OS8) was chosen for SK-OV-3 [14], EGFR (PDB ID: 5WB7) was chosen for SW-626 [15], androgen receptor (PDB ID: 2Q7I) was chosen for OVCAR3 [16], and Gonadotropin-releasing hormone (GnRH) receptor (PDB ID: 7BR3) was chosen for Caov-3 [17]. Moreover, the activity of these compounds against COVID-19 was assessed by investigating their interactions with COVID-19 RNA-dependent RNA polymerase (RdRP) (PDB ID: 7BZF) [18]. The chemical activities of Skullcapflavone I and Skullcapflavone II were evaluated against these proteins and enzymes. The 3D structure of the biomolecules was gained from the PDB database and prepared using the protein preparation module of the Schrödinger [19]. Finally, the system was minimized by applying the OPLS3e force field. To obtain more reliable results, the active site of the biomolecules was determined using the SiteMap of Schrödinger [18], and a receptor grid was produced around the active site. The compounds Skullcapflavone I and Skullcapflavone II were obtained from the PubChem database and prepared using the LigPrep module of Schrödinger [20]. Indeed, the in silico calculations were employed utilizing the Glide of Schrödinger suites [12]. The LigPreb output files that had been prepared were merged with redistribution for sub-jobs and utilized as input files for screening. The Epik state penalties were employed for docking, and the unique properties generated for each input compound were used to identify the unique compound. Calculations for docking with standard precision (SP) and extreme precision (XP) were completed. The flexible docking method was used, and after each step, 10% of the best postures with retention of all good scoring states were maintained. Scaling factor and partial charge cutoff values were respectively set at 0.80 and 0.15. Poses that have a strong enough link with the protein are allowed. The pose viewer was employed in the last phase to examine the interactions between particular ligands and protein docked complexes. The calculation of binding free energies was conducted utilizing the MM/GBSA method. The calculations were conducted using the Prime of Schrödinger. The force field and solvation model, meanwhile, were implemented using the VSGB and OPLS-2005, respectively. The free energy needed to bind a ligand to a protein has the following formula:

$$\Delta G\,\mathrm{bind} = G\,\mathrm{complex} - (G\,\mathrm{protein} + G\,\mathrm{ligand})$$

Cancer Assays

Replication of Cells

To investigate the anti-cancer activity of the Skullcapflavones I and II on ovarian cancer cell lines (SW-626, SK-OV-3, OVCAR3, and Caov-3) and normal (HUVEC) cell lines for analyzing of cytotoxicity were obtained from our lab group and used in the work. Cell flasks were maintained at 37 °C (Thermo Forma II CO_2 Incubator, USA) in an atmosphere with 5% CO_2 throughout the course of the experiment, and cells were fed twice per week. After being stained with 0.4% trypan blue, the confused cells were removed using a trypsin-EDTA solution and counted under a microscope [21].

Treatment with Test Compounds

The test chemicals were added at concentrations ranging from 1–300 µM to the cell-seeded wells, and the plates were then incubated for 24 h at 37 °C with 5% CO_2. The MTT technique was used to assess any potential impacts of the administered chemicals on cell viability at the conclusion of the incubation. In this study, we took measurements at different concentrations (1, 5, 10, 25, 50, 100, 200, 300 µL) and then calculated Statistical values and standard deviations [22].

MTT Method

This part was studied based on the previous studies [23].

Enzymes Assays

α-Glycosidase inhibitory effect of Skullcapflavones I and II was assessed using the *p*-nitrophenyl-D-glycopyranoside substrate produced utilizing the prior approach [24].

SDH Activities

The SDH activity of Skullcapflavones I and II was spectrophotometrically evaluated using dl-glyceraldehyde, taking into account the decrease of NADPH at 340 nm. This part was studied based on the previous studies [25].

α-Glycosidase and SDH Inhibition Assays

Different natural component concentrations were put into the reaction tube in order to track the impact of skullcap flavones I and II on -glycosidase and SDH. SDH activity was assessed prior to the creation of the control sample without the presence of any natural substances. The half maximal inhibitory activity (IC_{50}) was calculated from activity (%) versus some natural compounds concentration plots according to the previous studies [26].

Results and Discussion

Molecular Docking and MM/GBSA Results

The chemical activities of skullcapflavone I and skullcapflavone II when interacting with the enzymes (alpha glucosidase, sorbitol dehydrogenase, and RdRP) and proteins (estrogen receptor, EGFR, androgen receptor, and GnRH receptor) were estimated by conducting the molecular modeling analyses. The results revealed the residues of the biomolecules that can construct powerful interactions with the molecules. The modeling pose of skullcapflavone I among the residues of alpha glucosidase is shown in Fig. 1A. The interactions among skullcapflavone I and alpha glucosidase are shown in Fig. 1B. From Fig. 1B, it is observed that skullcapflavone I has created two H bonds with the residues of alpha glucosidase. These residues are Glu748 and Arg854. There are also eight hydrophobic factors, which rise the binding affinity of skullcapflavone I to studied enzyme. The residues of this part are His708, Leu712, Gln715, Glu721, Tyr822, Ile823, Gly855, and Glu856.

The modeling pose of skullcapflavone II among the residues of alpha glucosidase is shown in Fig. 1C, and their interactions are presented in Fig. 1D. Additionally, skullcapflavone II has created three hydrogen bonds with alpha glucosidase. These residues are Glu715, Arg854, and Glu856. The residues with hydrophobic contacts are His708, Leu712, Gly747, Glu748, Ala749, Tyr822, and Ile823.

Figure 2A shows the docking pose of skullcapflavone I among the residues of sorbitol dehydrogenase. The interactions among skullcapflavone I and the enzyme are seen in Fig. 2B. There are two hydrogen bonds among the molecule and the residues of sorbitol dehydrogenase, which are Thr202 and Asp203. There are also nine hydrophobic contacts with the residues Cys178, Gly179, Leu204, Arg208, Ile231, Thr250, Ala254, Ser255, and Ala258.

Figure 2C represents the modeling of skullcapflavone II among the residues of sorbitol dehydrogenase, and their interactions are seen in Fig. 2D. Skullcapflavone II has created three H bonds and nine hydrophobic factors with sorbitol dehydrogenase. The residues with hydrogen bonds are Thr202, Asp203, and Leu204, and the residues with hydrophobic contacts are Arg208, Ile223, Ser224, Glu226, Ile231, Thr250, Ala252, Ala254, and Ser255.

The docking pose of skullcapflavone I among the residues of SARS-CoV-2 RdRP is presented in Fig. 3A, and their interactions are displayed in Fig. 3B. Skullcapflavone I has created one hydrogen bond with the residues of RdRP, which is Pro677. This compound has created six hydrophobic contacts with RdRP residues. These residues are Arg249, Ser318, Arg349, Arg457, Leu460, and Pro461. Figure 3C displays the docking pose of Skullcapflavone II among the residues of SARS-CoV-2 RdRP, and the interactions are presented in Fig. 3D. There are two hydrogen bonds between Skullcapflavone II and RdRP. These residues are Arg349 and Pro677. There are also nine hydrophobic contacts between this compound and RdRP. These residues are Ile26, Thr27, His35, Glu37, Gly40, Glu75, Thr76, and Arg150. The docking pose of skullcapflavone I among the residues of estrogen receptor is displayed in Fig. 4A. Their interactions are presented in Fig. 4B. There are no hydrogen bonds between skullcapflavone I and the residues of the estrogen receptor. There are eleven hydrophobic contacts between skullcapflavone I and residues Leu346, Leu349, Glu353, Leu387,

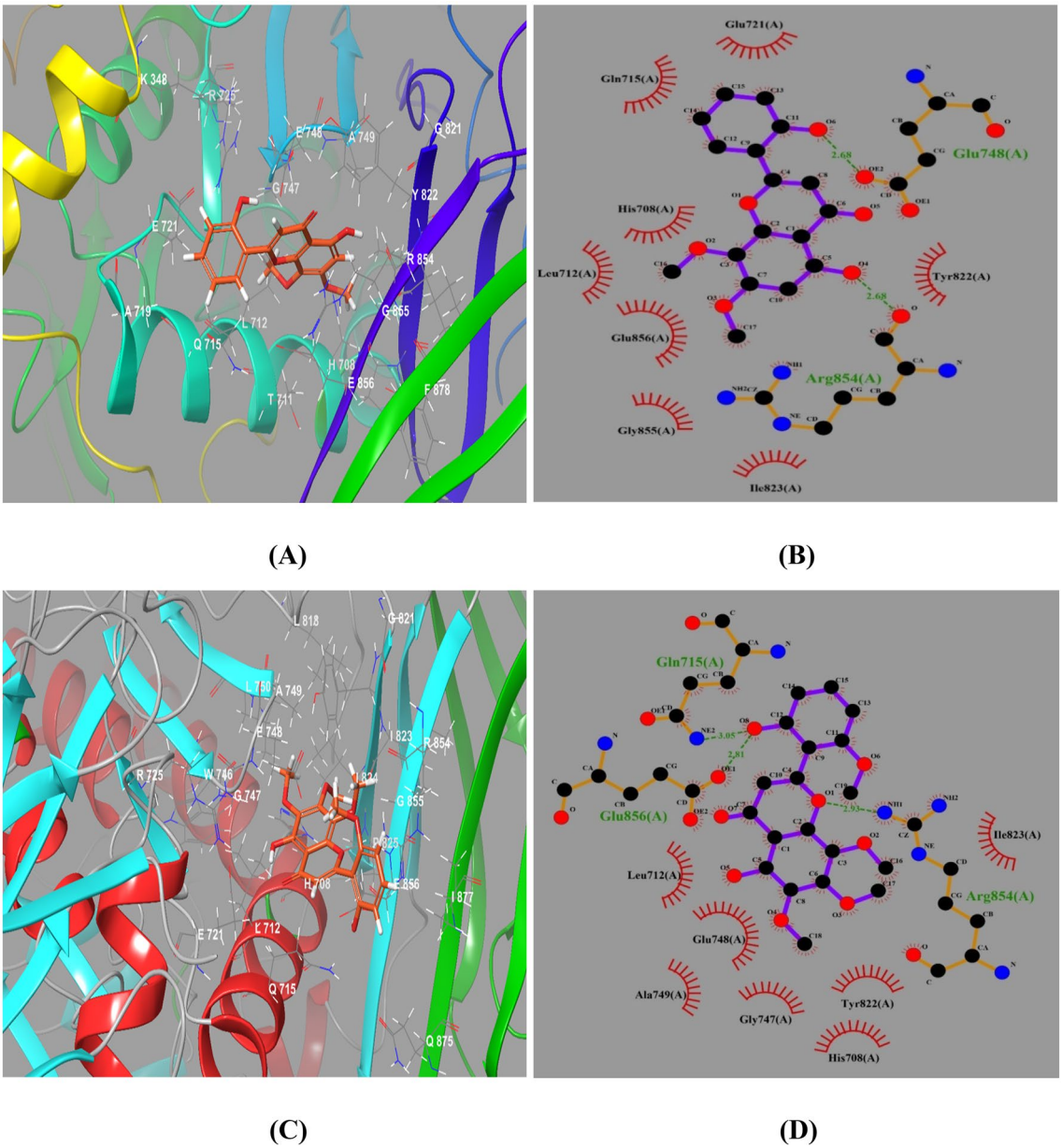

Fig. 1 **A** The docking pose of skullcapflavone I among α-glucosidase residues. **B** The interactions of skullcapflavone I and alpha glucosidase. **C** The docking pose of skullcapflavone II among alpha glucosidase. **D** The interactions of skullcapflavone II and alpha glucosidase

Met388, Phe404, Leu428, Leu391, Ile424, Met421, and Leu525.

The modeling pose of skullcapflavone II among the residues of estrogen receptor is seen in Fig. 4C, and their interactions are displayed in Fig. 4D. Like skullcapflavone I, skullcapflavone II has no H bonds with the residues of estrogen receptor. There are nine hydrophobic contacts between the molecule and the residues of estrogen receptor. These residues are Met388, Ile389, Val392, Met427, Ala430, Phe435, His513, His516, and Ser518. Figure 5A shows the docking pose of skullcapflavone I among the EGFR residues, and their interactions are seen in Fig. 5B. The results show that skullcapflavone I has created two H bonds with Leu38 and Asn86 and two hydrogen bonds with Tyr251. The residues that have created hydrophobic contact with skullcapflavone I are Val36, Glu60, Ala62, Arg84, Thr249, and Ala265.

The modeling pose of skullcapflavone II among the residues of androgen receptor is seen in Fig. 5C. The interactions between this compound and the EGFR residues are presented in Fig. 5D. Like skullcapflavone I, skullcapflavone II has constructed two hydrogen bonds with Leu38

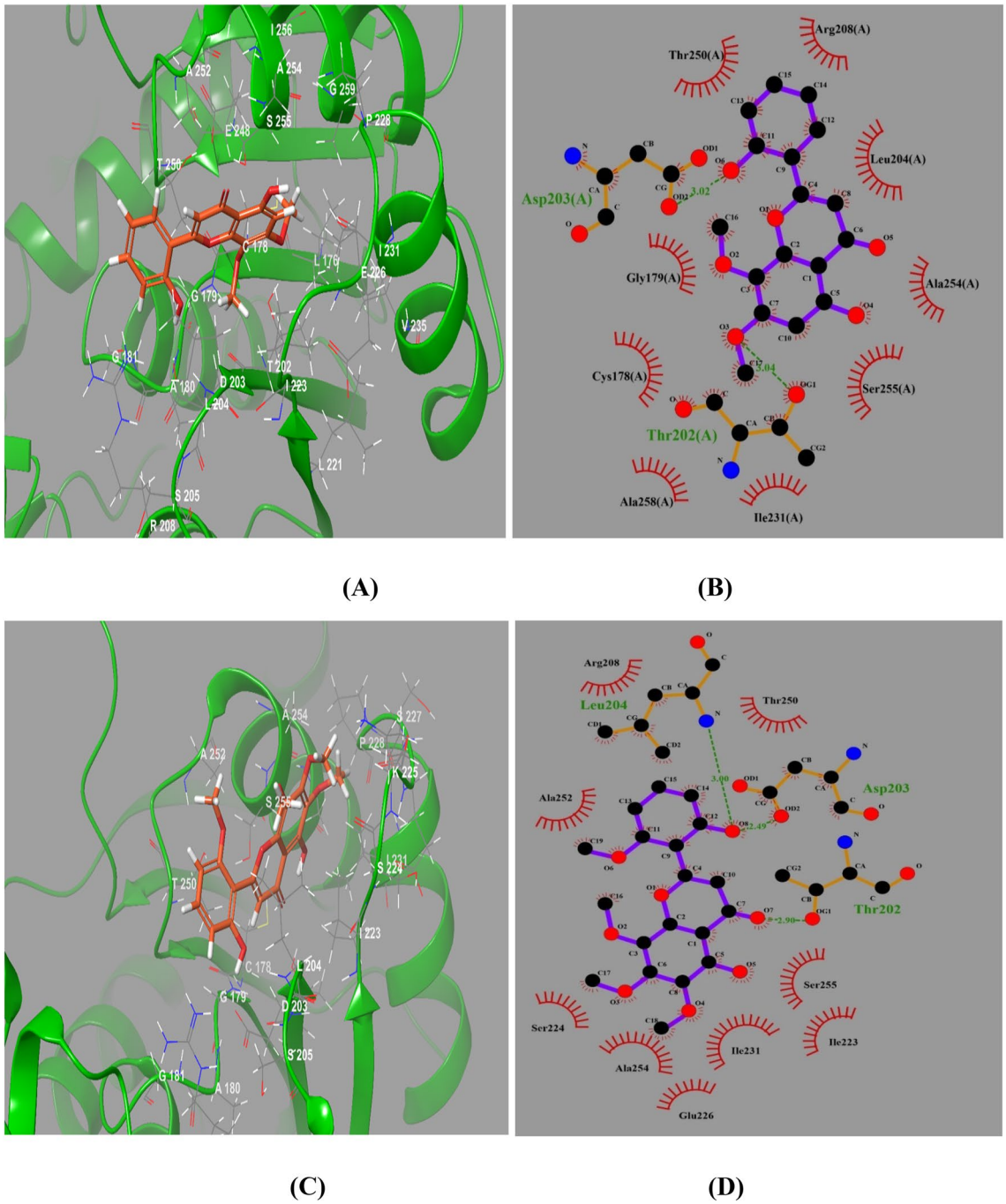

Fig. 2 **A** The docking pose of skullcapflavone I among sorbitol dehydrogenase. **B** The interactions of skullcapflavone I and sorbitol dehydrogenase. **C** The docking pose of skullcapflavone I among sorbitol dehydrogenase. **D** The interactions of skullcapflavone II and sorbitol dehydrogenase

and Asn86 and two hydrogen bonds with Tyr251. There are also five hydrophobic contacts between skullcapflavone II and the residues of EGFR. These residues are Glu60, Ala62, Arg84, Thr249, and Ala265. The modeling pose of skullcapflavone I among the residues of androgen receptor is seen in Fig. 6A. Their interactions are seen in Fig. 6B. There is one hydrogen bond between Skullcapflavone I and the androgen receptor. This residue is Val685. There are thirteen hydrophobic contacts between skullcapflavone I and residues Glu681, Pro682, Gly683, Val684, Gln711, Val715, Trp718, Leu744, Met745, Ala748, Arg752, Phe804, and Lys808. These numerous hydrophobic contacts can enhance the binding affinity of this compound considerably.

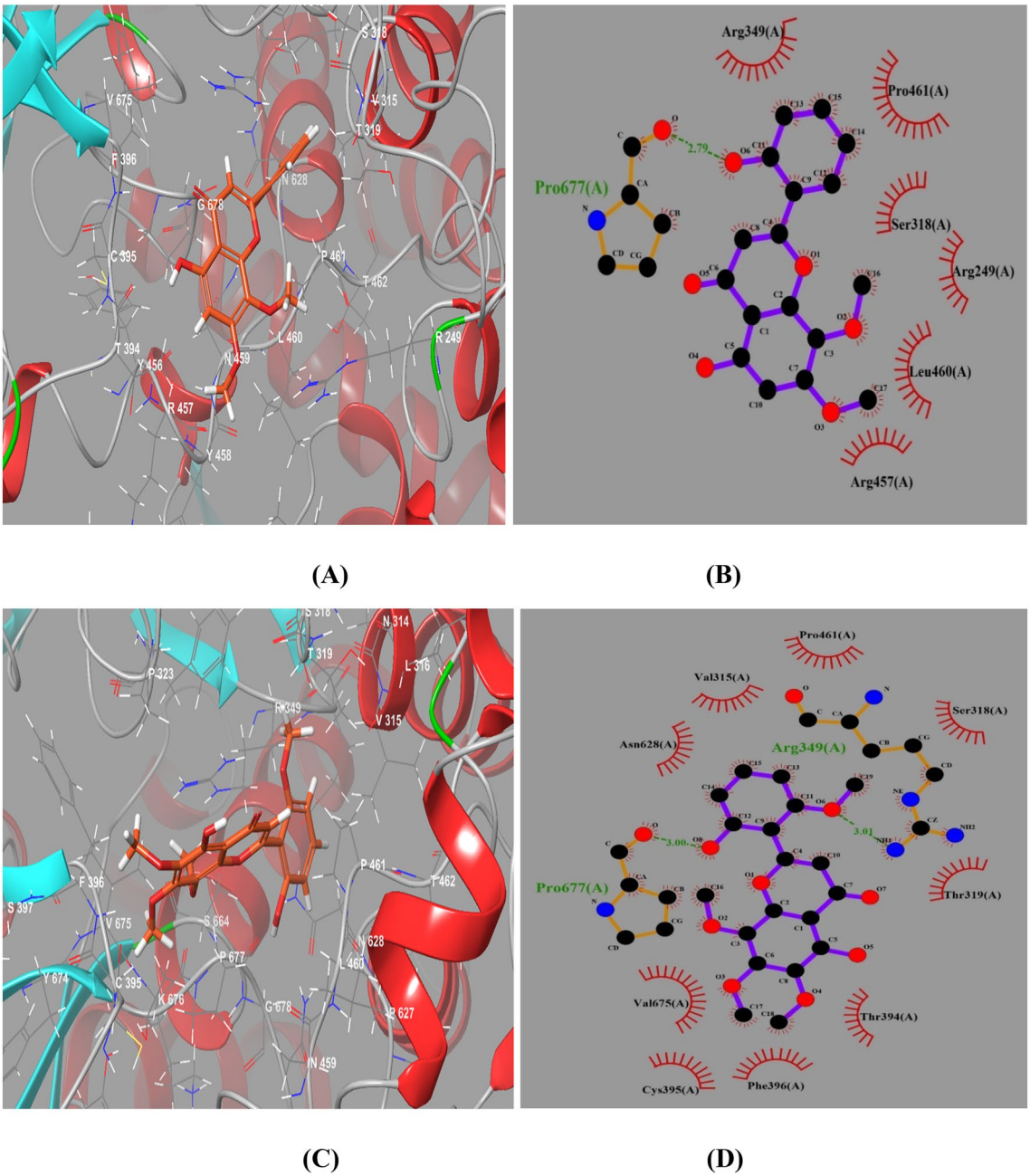

Fig. 3 **A** The docking pose of skullcapflavone I among SARS-CoV-2 RdRP residues. **B** The interactions of skullcapflavone I and SARS-CoV-2 RdRP. **C** The docking pose of skullcapflavone II among SARS-CoV-2 RdRP residues. **D** The interactions of skullcapflavone II and SARS-CoV-2 RdRP

The docking pose of skullcapflavone II among the residues of androgen receptor is presented in Fig. 6C, and their interactions are displayed in Fig. 6D. Skullcapflavone II has one hydrogen bond with the residue Val685 of the estrogen receptor. There are eleven hydrophobic contacts between the compound and the residues of the androgen receptor. These residues are Glu681, Pro682, Gly683, Val684, Gln711, His714, Val715, Ala748, Arg752, Asn756, and Lys808.

Figure 7A shows the docking pose of skullcapflavone I among the residues of GnRH receptor. The interactions between skullcapflavone I and the protein are presented in Fig. 7B. There is no hydrogen bond between the compound and the residues of the GnRH receptor. There are eleven hydrophobic contacts with the residues Ile21, Pro22, Leu23, Asn27, Phe216, Leu219, Tyr283, Leu286, Gly287, Tyr290, and Leu297. Figure 7C represents the docking pose of skullcapflavone II among the residues of the GnRH receptor, and

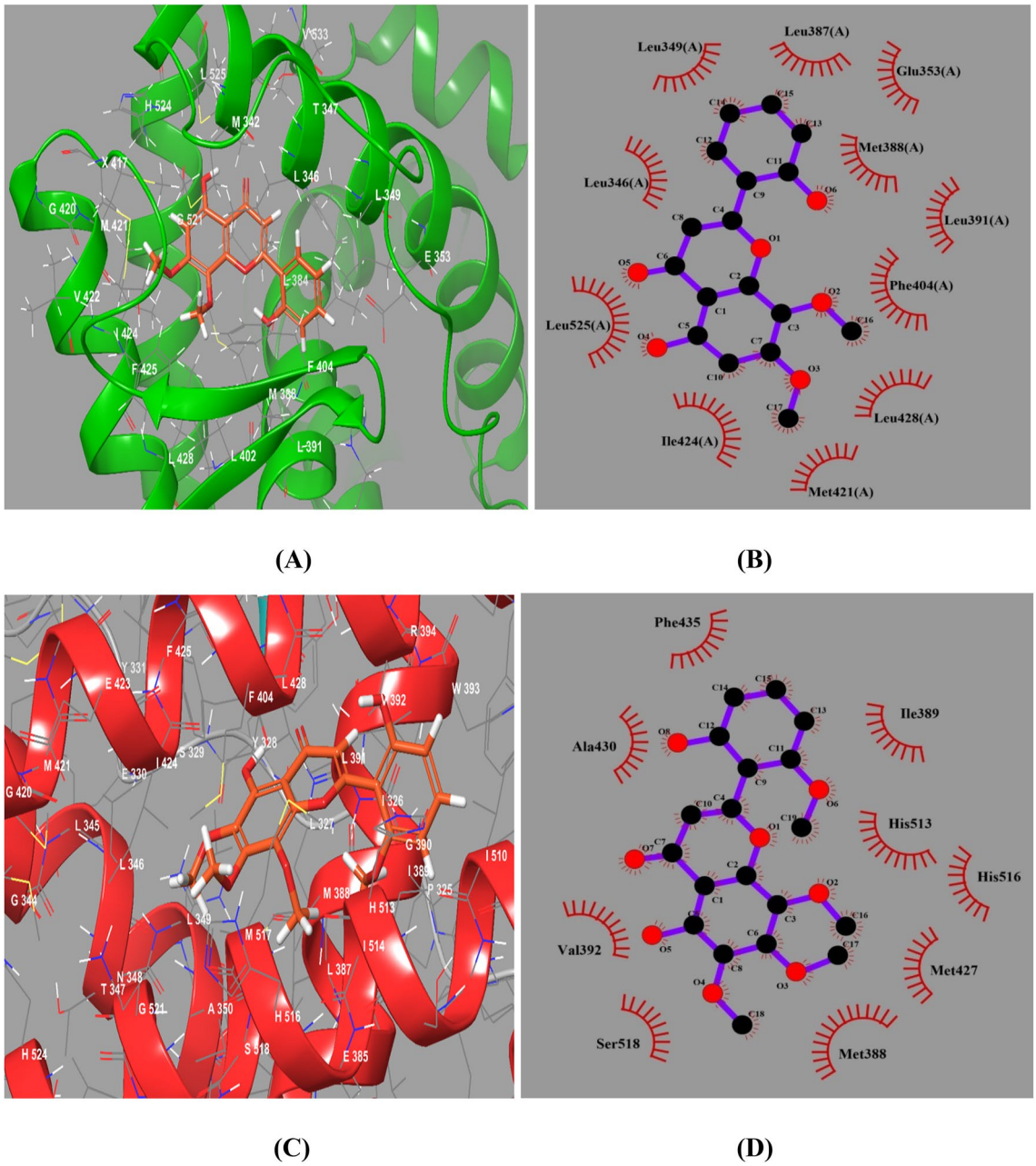

Fig. 4 **A** The docking pose of skullcapflavone I among estrogen receptor residues. **B** The interactions of skullcapflavone I and estrogen receptor. **C** The docking pose of skullcapflavone II among estrogen receptor residues. **D** The interactions of skullcapflavone II and estrogen receptor

their interactions are presented in Fig. 7D. Skullcapflavone II has created three hydrogen bonds and ten hydrophobic contacts with the residues of the GnRH receptor. The residues with hydrogen bonds are Lys121, Tyr283, and Asn305, and the residues with hydrophobic contacts are Ile21, Pro22, Leu23, Gln25, Gly26, Asp98, Met125, Phe216, Leu219, and Gly287.

In addition to determining the potential interactions between the compounds and biomolecules, the molecular docking analysis can specify the binding affinity of the ligands to the enzymes or proteins. The docking score indicates this affinity. The docking scores, the length of hydrogen bonds, and the binding free energies for the ligand–enzyme and ligand–protein complexes discussed above are displayed in Tables 1 and 2. As can be seen in Table 1, the IC50 of Skullcapflavone I has a positive correlation with docking scores against α-glucosidase and sorbitol dehydrogenase. It means when the binding affinity increases, the inhibitory activity against these enzymes increases too. This trend has also happened for Skullcapflavone II. When

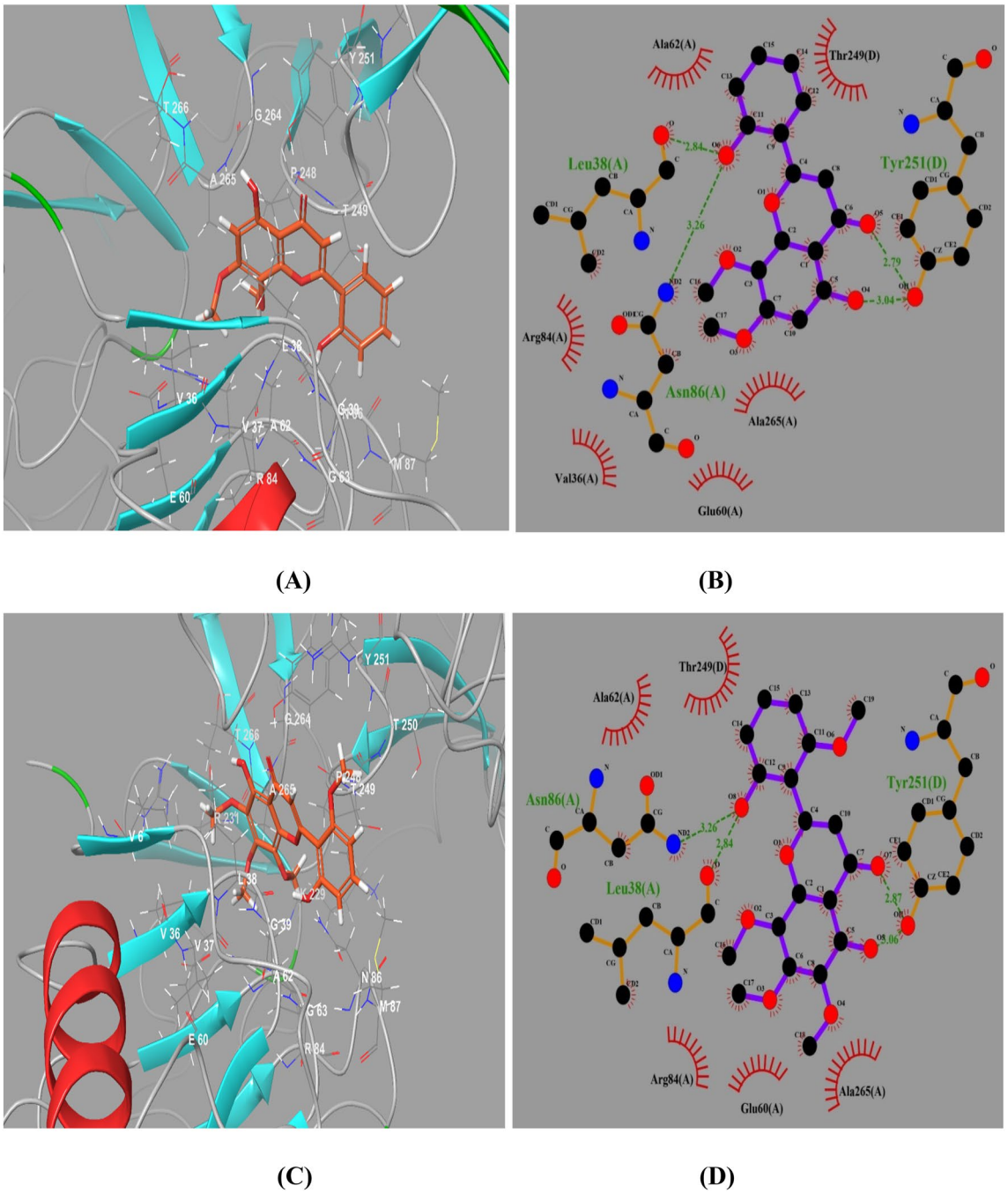

Fig. 5 **A** The modeling pose of skullcapflavone I among EGFR residues. **B** The interactions of skullcapflavone I and EGFR. Semicircles show the hydrophobic contacts and green dashed lines indicate the hydrogen bonds. **C** The modeling pose of skullcapflavone II among EGFR residues. **D** The interactions of skullcapflavone II and EGFR

the docking score for this compound against α-glucosidase and sorbitol dehydrogenase decreased from − 4.094 kcal/mol to − 6.304 kcal/mol, the IC50 decreased from 95.04 μM to 28.81 μM. Tis correlation indicates the reliability of the obtained results. Interestingly, this correlation has also happened for the binding free energies. In general, this trend could be seen for the receptors in cancer cell lines. Therefore it could be concluded that the selected receptors in these cancer cells are probable targets of the studied compounds. Although skullcapflavone I and skullcapflavone II are practical inhibitors against these enzymes and proteins, these compounds have to be delivered to the target site. An adequate solution for this problem is vesicular nanocarriers [27, 28].

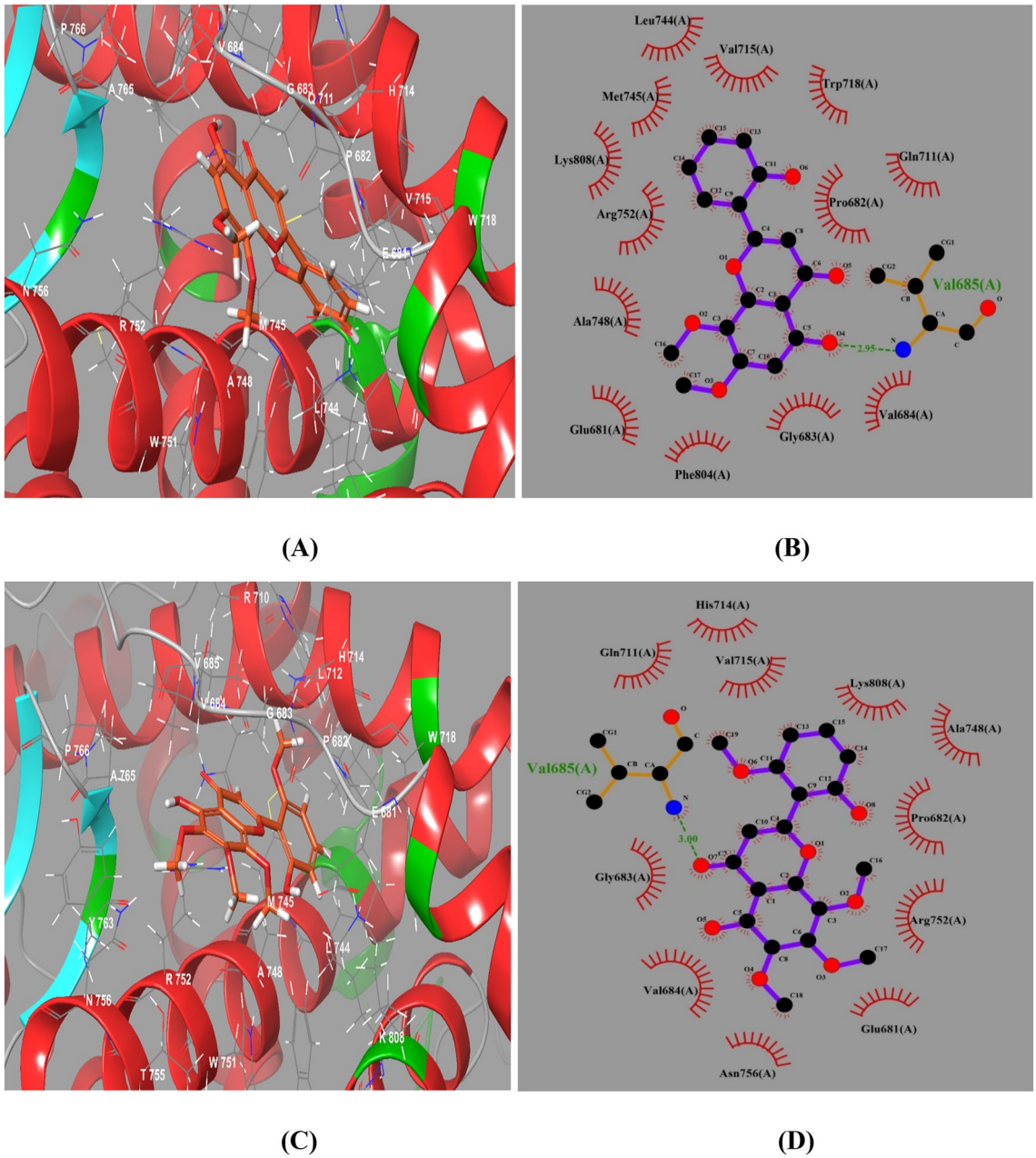

Fig. 6 **A** The docking pose of skullcapflavone I among androgen receptor residues. **B** The interactions of skullcapflavone I and androgen receptor. **C** The docking pose of skullcapflavone II among androgen receptor residues. **D** The interactions of skullcapflavone II and androgen receptor

Enzymes Results

Sorbitol dehydrogenase inhibitor compounds have been recorded to alleviate or prevent, diverse secondary complications of diabetes mellitus [29]. Recently, it has been established that the most effective treatment for type 2 diabetes for regulating postprandial hyperglycemia and associated harmful biological sequelae is the use of bioactive-glucosidase inhibitor substances [30]. The α-glucosidase enzyme is competitively inhibited by the α-glucosidase inhibitors that controlled the postprandial hyperglycemia [31]. In this study, Skullcapflavone I and Skullcapflavone II compounds showed excellent to good inhibitory activities against α-glucosidase and sorbitol dehydrogenase enzymes with IC50 values of 102.66 ± 8.43 and 95.04 ± 11.52 nM for α-glucosidase and 38.42 ± 3.82 and 28.81 ± 3.26 nM for sorbitol dehydrogenase. In this study, the inhibition effects of these phenolic compounds on two important enzymes were investigated and their anti-diabetic capacity was determined by different methods. The outcomes were evaluated against the reference

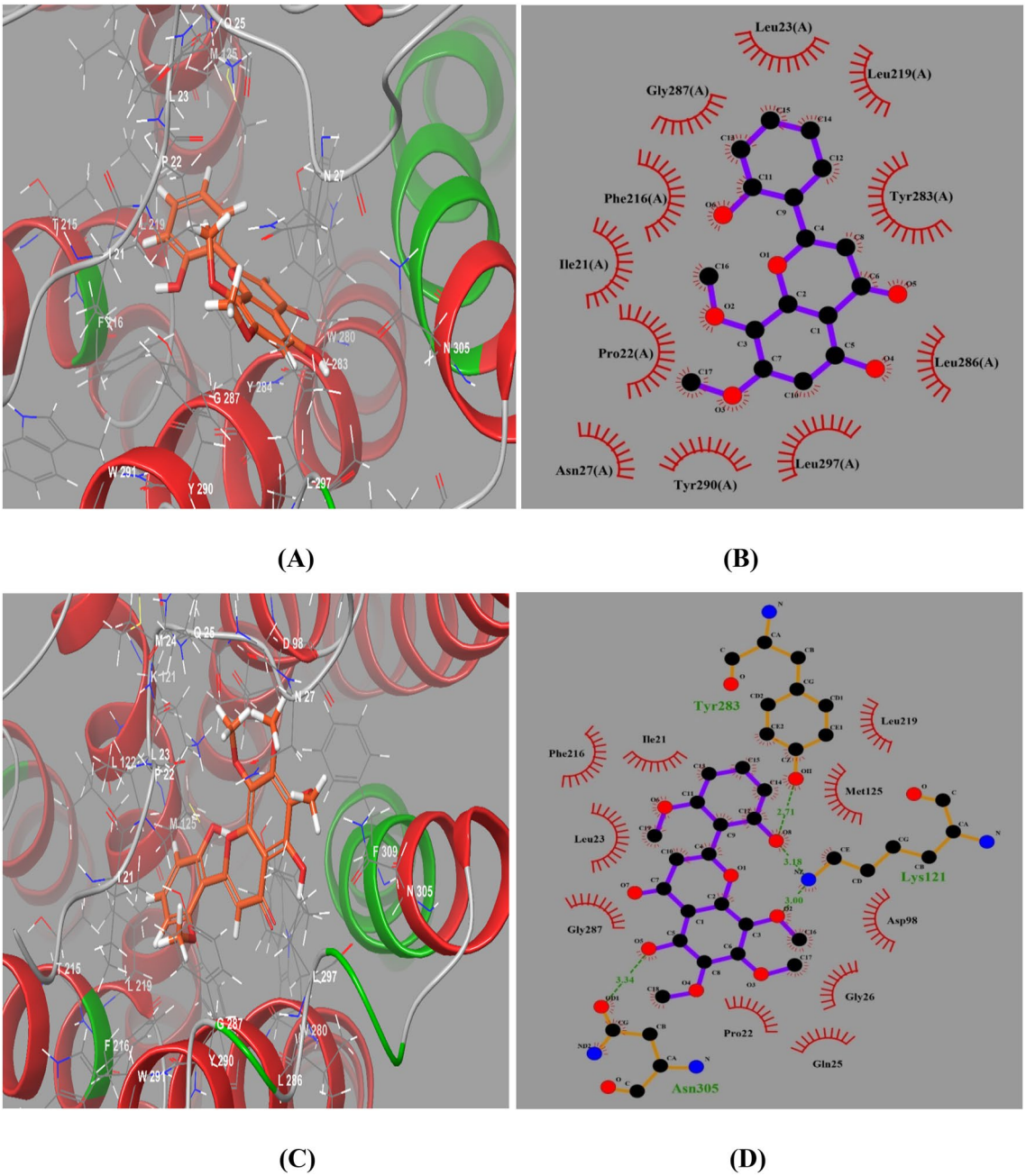

Fig. 7 **A** The docking pose of skullcapflavone I among GnRH receptor residues. **B** The interactions of skullcapflavone I and GnRH receptor. The semicircles show the hydrophobic contacts. **C** The docking pose of skullcapflavone II among GnRH receptor residues. **D** The interactions of skullcapflavone II and GnRH receptor

molecule utilized in the relevant activities. Future biochemical, physiological, and pharmacological investigations in the relevant domains will undoubtedly benefit from the findings, and they will also have a significant impact on the understanding and management of numerous metabolic illnesses, including diabetes. In this connection, it is anticipated that two natural compounds would significantly influence the creation of pharmaceuticals for future usage in treatment and associated applications. In this study, the results of natural substances were obtained at a good level compared to acarbose standard compound.

Anticancer Results

The cytotoxic effect of Skullcapflavone I and Skullcapflavone II on ovarian cancer cell lines is shown in Table 3.

Table 1 The docking scores, total binding free energy, and the length of H-bonds obtained from the molecular docking calculations of Skullcapflavone I and Skullcapflavone II against the enzymes

Compound	Parameter	α-glucosidase	Sorbitol dehydrogenase	RdRP
Skullcapflavone I	IC_{50} (nM)	102.66	38.42	–
	Docking score (kcal/mol)	− 3.420	− 5.611	− 5.033
	Total binding free energy (kcal/mol)	− 34.97	− 58.24	− 45.82
	Residues with H-bond and their length	Glu748:2.68 Å	Thr202: 3.04 Å	Pro677:2.79 Å
		Arg854:2.68 Å	Asp203: 3.02 Å	
Skullcapflavone II	IC_{50} (μM)	95.04	28.81	–
	Docking score (kcal/mol)	− 4.094	− 6.304	− 5.408
	Total binding free energy (kcal/mol)	− 50.37	− 57.95	− 52.54
	Residues with H-bond and their length	Gln715: 3.05 Å	Thr202: 2.90 Å	Arg349:3.01 Å
		Arg854: 2.93 Å	Asp203: 2.49 Å	Pro677:3.00 Å
		Glu856: 2.81 Å	Leu204: 3.00 Å	

Table 2 The docking scores, total binding free energy, and the length of H-bonds obtained from the molecular docking calculations of Skullcapflavone I and Skullcapflavone II against the surface receptors

Compound	Parameter	Estrogen receptor (SK-OV-3)	EGFR (SW-626)	Androgen receptor (OVCAR3)	GnRH (Caov-3)
Skullcapflavone I	IC_{50} (μM)	63.14	1.55	19.42	52.04
	Docking score (kcal/mol)	− 9.591	− 7.249	− 5.182	− 8.359
	Total binding free energy (kcal/mol)	− 72.34	− 58.97	− 58.98	− 50.42
	Residues with H-bond and their length	–	Leu38:2.84 Å	Val685:2.95 Å	–
			Asn86:3.26 Å		
			Tyr251:2.79 Å		
			Tyr251:3.04 Å		
Skullcapflavone II	IC_{50} (μM)	5.18	21.44	33.87	72.66
	Docking score (kcal/mol)	− 8.643	− 7.821	− 5.210	− 8.001
	Total binding free energy (kcal/mol)	− 68.12	− 67.50	− 50.89	− 60.60
	Residues with H-bond and their length	–	Leu38: 2.84 Å	Val685:3.00 Å	Lys121:3.00 Å
			Asn86: 3.26 Å		Lys121:3.18 Å
			Tyr251:2.87 Å		Tyr283:2.71 Å
			Tyr251:3.06 Å		Asn305:3.34 Å

Table 3 In vitro anti-proliferative activities of Skullcapflavone I and Skullcapflavone II compounds against ovarian cancer cell lines

No	Compounds	SK-OV-3 IC_{50} (μM)[c]	SW-626 IC_{50} (μM) [c]	OVCAR3 IC_{50} (μM)[c]	Caov-3 IC_{50} (μM)[c]	IOSE80[a] IC_{50} (μM)[c]	SI[b] IC_{50} (μM)[c]
1	Skullcapflavone I	63.14 ± 4.18	1.55 ± 0.05	19.42 ± 0.97	52.04 ± 6.14	71.88 ± 6.05	1.13
2	Skullcapflavone II	5.18 ± 1.02	21.44 ± 3.23	33.87 ± 7.05	72.66 ± 5.48	31.21 ± 3.07	6.02
	Paclitaxel[d]	80.12 ± 10.02	32.52 ± 4.60	34.32 ± 6.02	64.62 ± 8.25	91.68 ± 9.48	1.14

[a]Normal ovarian epithelial cells (IOSE80)

[b]SI (Selectivity Index) = IC50 values on IOSE80 cells/SK-OV-3 cells

[c]The IC50 reported was determined using the MTT method

[d]Paclitaxel was taken as reference

Low dosages of the substances skullcapflavones I and II greatly reduced ovarian cancer cell viability (Table 3; n:3). Skullcapflavone I compound had cytotoxicity impacts with IC50 values of 63.14 µM for SK-OV-3 cell line, 1.55 µM for SW-626, 19.42 µM for OVCAR3 cell line, and 52.04 µM for Caov-3 cell line, respectively. Additionally, the viability of ovarian cancer cells was significantly decreased by a 300 µM dosage of all substances. Skullcapflavone I and Skullcapflavone II show cytotoxic effects in all cell types, and this impact is most potent in ovarian cancer cell lines, according to our general assessment of the two studied substances (SK-OV-3, SW-626, OVCAR3, Caov-3). Additionally, Skullcapflavone II compound had cytotoxicity impacts with IC50 values of 5.18 µM for SK-OV-3 cell line, 21.44 µM for SW-626, 33.87 µM for OVCAR3 cell line, and 72.66 µM for Caov-3 cell line, respectively. For instance, Makaluvamine Analog FBA-TPQ strongly suppressed the growth of ovarian cancer cells A2780 and OVCAR-3 in one study, with IC50 values of 1.78 and 0.98 µM, respectively [32]. These results were similar to the results of our study, we plan to study these natural compounds in vivo in our future studies. In the last decade, intensive studies have been carried out to treat the disease by intervening at the gene level with gene therapy methods. New approaches are being developed in the treatment of rare diseases, cancer, viral infections, cardiovascular diseases, and nervous tissue disorders by using various gene therapy methods. Previous research have shown that doxorubicin and Bcl2 siRNA combination therapy enhances apoptosis of SK-OV-3 ovarian cancer cells to increase drug sensitivity, although only some cancer cell lines are drug-sensitive while others are not. However, currently approved therapies are not yet available.

Conclusions

Accordingly, in recent updates on the treatment of diabetes, α-glucosidase inhibitors (Skullcapflavone I and Skullcapflavone II in this study had values of 95 and 102 nM) from various plant sources due to their ability to inhibit α-glucosidase activity. To slow down the hydrolytic cleavage of dietary oligosaccharides' non-reducing end and the release of -glucose, which postpones the breakdown of carbohydrates and the absorption of glucose in the small intestine. One of the current therapeutic strategies for maintaining blood glucose levels in diabetic patients, notably in T2D, this mechanism is crucial in regulating postprandial hyperglycemia. Acarbose, voglibose, miglitol, and migration are examples of antidiabetic medications with alpha-glucosidase inhibitory characteristics that are currently commercially accessible to manage postprandial hyperglycemia. However, regular use of these drugs leads to various side effects such as severe stomach pain, vomiting, bloating, diarrhea, and allergic reactions. To evaluate the results of experimental research, in silico approaches can be used as useful tools. These techniques can provide an interpretation of the interactions in a more explicit view. In this work, molecular modeling was used to examine the activities of skullcapflavone I and skullcapflavone II against α-glucosidase and sorbitol dehydrogenase. The activities of these compounds were also investigated against four expressed surface receptor proteins (estrogen receptor, EGFR, androgen receptor, and GnRH receptor) in the cancer cell lines SW-626, SK-OV-3, OVCAR3, and Caov-3. The activity of the compounds was also investigated against RdRP of SARS-COV-2. The outcomes revealed that skullcapflavone I and skullcapflavone II could be regarded as possible inhibitors for the mentioned enzymes and cancer cell lines.

Funding Shenzhen Baoan District Science and Technology Innovation Bureau, Grant No. 2021JD148.

Declarations

Conflict of interest The authors declare that they have no conflict of interest.

References

1. Gong, W.-Y., Wu, J.-F., Liu, B.-J., Zhang, H.-Y., Cao, Y.-X., Sun, J., Lv, Y.-B., Wu, X., & Dong, J.-C. (2014). Flavonoid components in Scutellaria baicalensis inhibit nicotine-induced proliferation, metastasis and lung cancer-associated inflammation in vitro. *International Journal of Oncology, 44*(5), 1561–1570.
2. Zhao, Z., Liu, B., Sun, J., Lu, L., Liu, L., Qiu, J., Li, Q., Yan, C., Jiang, S., Mohammadtursun, N., Ma, W., Li, M., Dong, J., & Gong, W. (2019). Scutellaria flavonoids effectively inhibit the malignant phenotypes of non-small cell lung cancer in an Id1-dependent manner. *International Journal of Biological Sciences, 15*(7), 1500.
3. Kim, S. H., Jo, S. H., Kwon, Y. I., & Hwang, J. K. (2011). Effects of onion (*Allium cepa* L.) extract administration on intestinal α-glucosidases activities and spikes in postprandial blood glucose levels in SD rats model. *International Journal of Molecular Sciences, 12*(6), 3757–3769.
4. Lindstad, R. I., Teigen, K., & Skjeldal, L. (2013). Inhibition of sorbitol dehydrogenase by nucleosides and nucleotides. *Biochemical and Biophysical Research Communications, 435*(2), 202–208.
5. Palanisamy, C. P., Cui, B., Zhang, H., Panagal, M., Paramasivam, S., Chinnaiyan, U., Jeyaraman, S., Murugesan, K., Rostagno, M., Sekar, V., & Natarajan, S. P. (2021). Anti-ovarian cancer potential of phytocompound and extract from South African medicinal plants and their role in the development of chemotherapeutic agents. *American Journal of Cancer Research, 11*(5), 1828.
6. Wang, C.-W., Chen, C.-L., Wang, C.-K., Chang, Y.-J., Jian, J.-Y., Lin, C.-S., Tai, C.-J., & Tai, C.-J. (2015). Cisplatin-, doxorubicin-, and docetaxel-induced cell death promoted by the aqueous extract of *Solanum nigrum* in human ovarian carcinoma cells. *Integrative Cancer Therapies, 14*(6), 546–555.
7. Mihăşan, M. (2012). What in silico molecular docking can do for the 'bench-working biologists.' *Journal of Biosciences, 37*(1), 1089–1095.

8. Chandrika, B. R., Subramanian, J., & Sharma, S. D. (2009). Managing protein flexibility in docking and its applications. *Drug Discovery Today, 14*(7–8), 394–400.
9. Meng, X. Y., Zhang, H. X., Mezei, M., & Cui, M. (2011). Molecular docking: A powerful approach for structure-based drug discovery. *Current Computer-Aided Drug Design, 7*(2), 146–157.
10. Poustforoosh, A., Hashemipour, H., Pardakhty, A., & Pour, M. K. (2022). Preparation of nano-micelles of meloxicam for transdermal drug delivery and simulation of drug release: A computational supported experimental study. *The Canadian Journal of Chemical Engineering, 100*(11), 3428–3436.
11. Fan, J., Fu, A., & Zhang, L. (2019). Progress in molecular docking. *Quantitative Biology, 7*(2), 83–89.
12. Mehrabani, M., Raeiszadeh, M., Najafipour, H., EsmaeliTarzi, M., Amirkhosravi, A., Poustforoosh, A., Mohammadi, M. A., Naghdi, S., & Mehrabani, M. (2020). Evaluation of the cytotoxicity, antibacterial, antioxidant, and anti-inflammatory effects of different extracts of *Punica granatum* var. pleniflora. *Journal of Kerman University of Medical Sciences, 27*(5), 414–425.
13. Poustforoosh, A., Faramarz, S., Nematollahi, M. H., Hashemipour, H., Tüzün, B., Pardakhty, A., & Mehrabani, M. (2022). 3D-QSAR, molecular docking, molecular dynamics, and ADME/T analysis of marketed and newly designed flavonoids as inhibitors of Bcl-2 family proteins for targeting U-87 glioblastoma. *Journal of Cellular Biochemistry, 123*(2), 390–405.
14. Hua, W., Christianson, T., Rougeot, C., Rochefort, H., & Clinton, G. M. (1995). SKOV3 ovarian carcinoma cells have functional estrogen receptor but are growth-resistant to estrogen and antiestrogens. *The Journal of steroid Biochemistry and Molecular Biology, 55*(3–4), 279–289.
15. Puvanenthiran, S., Essapen, S., Seddon, A. M., & Modjtahedi, H. (2016). Impact of the putative cancer stem cell markers and growth factor receptor expression on the sensitivity of ovarian cancer cells to treatment with various forms of small molecule tyrosine kinase inhibitors and cytotoxic drugs. *International Journal of Oncology, 49*(5), 1825–1838.
16. Hamilton, T. C., Young, R. C., McKoy, W. M., Grotzinger, K. R., Green, J. A., Chu, E. W., Whang-Peng, J., Rogan, A. M., Green, W. R., & Ozols, R. F. (1983). Characterization of a human ovarian carcinoma cell line (NIH: OVCAR-3) with androgen and estrogen receptors. *Cancer Research, 43*(11), 5379–5389.
17. Cheung, L. W., Yung, S., Chan, T. M., Leung, P. C., & Wong, A. S. (2013). Targeting gonadotropin-releasing hormone receptor inhibits the early step of ovarian cancer metastasis by modulating tumor-mesothelial adhesion. *Molecular Therapy, 21*(1), 78–90.
18. Poustforoosh, A., Hashemipour, H., Tüzün, B., Pardakhty, A., Mehrabani, M., & Nematollahi, M. H. (2021). Evaluation of potential anti-RNA-dependent RNA polymerase (RdRP) drugs against the newly emerged model of COVID-19 RdRP using computational methods. *Biophysical Chemistry, 272*, 106564.
19. Schrödinger Release 2020-4: Protein Preparation Wizard; Epik, Schrödinger, LLC, New York, NY 2016; Impact, Schrödinger, LLC, New York, NY 2016; Prime, Schrödinger, LLC, New York, NY 2020.
20. Schrödinger Release 2020-4: LigPrep, Schrödinger, LLC, New York, NY 2020.
21. Pillay, N., Tighe, A., Nelson, L., Littler, S., Coulson-Gilmer, C., Bah, N., Golder, A., Bakker, B., Spierings, D. C. J., James, D. I., Smith, K. M., Jordan, A. M., Morgan, R. D., Ogilvie, D. J., Foijer, F., Jackson, D. A., & Taylor, S. S. (2019). DNA replication vulnerabilities render ovarian cancer cells sensitive to poly (ADP-ribose) glycohydrolase inhibitors. *Cancer Cell, 35*(3), 519–533.
22. Wu, Y. H., Huang, Y. F., Chen, C. C., Huang, C. Y., & Chou, C. Y. (2020). Comparing PI3K/Akt inhibitors used in ovarian cancer treatment. *Frontiers in Pharmacology, 11*, 206.
23. Guo, R., Liu, Q., Wang, W., Tayebee, R., & Mollania, F. (2021). Boron nitride nanostructures as effective adsorbents for melphalan anti-ovarian cancer drug. Preliminary MTT assay and in vitro cellular toxicity. *Journal of Molecular Liquids, 325*, 114798.
24. Lawag, I. L., Aguinaldo, A. M., Naheed, S., & Mosihuzzaman, M. (2012). α-Glucosidase inhibitory activity of selected Philippine plants. *Journal of Ethnopharmacology, 144*(1), 217–219.
25. Kazeem, M. I., Umukoro, O. G., Ogunrinola, O. O., Nafiu, M. O., & Akanji, M. A. (2021). Leafy vegetables inhibit activities of aldose reductase and sorbitol dehydrogenase in vitro. *International Journal of Vegetable Science, 27*(6), 552–560.
26. Kim, K. T., Rioux, L. E., & Turgeon, S. L. (2014). Alpha-amylase and alpha-glucosidase inhibition is differentially modulated by fucoidan obtained from *Fucus vesiculosus* and *Ascophyllum nodosum*. *Phytochemistry, 98*, 27–33.
27. Poustforoosh, A., Nematollahi, M. H., Hashemipour, H., & Pardakhty, A. (2022). Recent advances in bio-conjugated nanocarriers for crossing the blood-brain barrier in (pre-) clinical studies with an emphasis on vesicles. *Journal of Controlled Release*, *343*, 777–797. https://doi.org/10.1016/j.jconrel.2022.02.015
28. Asadikaram, G., Poustforoosh, A., Pardakhty, A., Torkzadeh-Mahani, M., & Nematollahi, M. H. (2021). Niosomal virosome derived by vesicular stomatitis virus glycoprotein as a new gene carrier. *Biochemical and Biophysical Research Communications, 534*, 980–987.
29. El-Kabbani, O., Darmanin, C., & Chung, R. T. (2004). Sorbitol dehydrogenase: Structure, function and ligand design. *Current Medicinal Chemistry, 11*(4), 465–476.
30. Hossain, U., Das, A. K., Ghosh, S., & Sil, P. C. (2020). An overview on the role of bioactive α-glucosidase inhibitors in ameliorating diabetic complications. *Food and Chemical Toxicology, 145*, 111738.
31. Williams, S. J., & Goddard-Borger, E. D. (2020). α-glucosidase inhibitors as host-directed antiviral agents with potential for the treatment of COVID-19. *Biochemical Society Transactions, 48*(3), 1287–1295.
32. Chen, T., Xu, Y., Guo, H., Liu, Y., Hu, P., Yang, X., Li, X., Ge, S., Velu, S. E., Nadkarni, D. H., Wang, W., Zhang, R., & Wang, H. (2011). Experimental therapy of ovarian cancer with synthetic makaluvamine analog: in vitro and in vivo anticancer activity and molecular mechanisms of action. *PLoS ONE, 6*(6), e20729.